Langmuir
Article
pubs.acs.org/Langmuir

Lateral Force Calibration: Accurate Procedures for Colloidal Probe Friction Measurements in Atomic Force Microscopy

Koo-Hyun Chung, Jon R. Pratt, and Mark G. Reitsma*

National Institute of Standards and Technology, 100 Bureau Drive, Gaithersburg, Maryland 20899

Received July 9, 2009. Revised Manuscript Received August 12, 2009

The colloidal probe technique for atomic force microscopy (AFM) has allowed the investigation of an extensive range of surface force phenomena, including the measurement of frictional (lateral) forces between numerous materials. The quantitative accuracy of such friction measurements is often debated, in part due to a lack of confidence in existing calibration strategies. Here we compare three in situ AFM lateral force calibration techniques using a single colloidal probe, seeking to establish a foundation for quantitative measurement by linking these techniques to accurate force references available at the National Institute of Standards and Technology. We introduce a procedure for calibrating the AFM lateral force response to known electrostatic forces applied directly to the conductive colloidal probe. In a second procedure, we apply known force directly to the colloidal probe using a precalibrated piezo-resistive reference cantilever. We found agreement between these direct methods on the order of 2% (within random uncertainty for both measurements). In a third procedure, we performed a displacement-based calibration using the piezo-resistive reference cantilever as a stiffness reference artifact. The method demonstrated agreement on the order of 7% with the direct force methods, with the difference attributed to an expected systematic uncertainty, caused by in-plane deflection in the cantilever during loading. The comparison establishes the existing limits of instrument accuracy and sets down a basis for selection criteria for materials and methods in colloidal probe friction (lateral) force measurements via atomic force microscopy.

1. Introduction

The atomic force microscope (AFM) has been used extensively as a measurement tool for the investigation of microscale to nanoscale interfacial forces. In the force measurement application known as the "colloidal probe" technique, a microscale sphere (glued to an AFM cantilever) is used to probe an interface instead of the usual integrated cantilever tip.[1] As integrated tips are typically limited in composition to either silicon or silicon nitride and because the contact area between a tip and surface can be very small, the alternative choice of a microscale colloidal probe can allow the user access to a much smaller stress regime and a broader choice of probe materials. This has allowed the investigation of a variety of surface force phenomena, where the potential for combinations of materials and environments is seemingly enormous.[2] The colloidal probe application has also found frequent use in the study of tribological phenomena for a similar variety of materials and environments.[3−8] This paper focuses on the AFM friction measurement technique called lateral force microscopy (LFM) using colloidal probes.

Figure 1 shows a front-view illustration (looking from the free end down the long axis of the colloidal probe cantilever) of a typical LFM measurement, in which force is applied in the y-direction and the cantilever twists about its long (x) axis. The quadrant position sensitive photodetector (PSD) of the AFM is also shown in Figure 1 with axes for normal (V_N) and lateral (V_L) output reading flexural and torsional deflection in the cantilever, respectively. Typical friction data for an LFM experiment are also illustrated in Figure 1, in which frictional energy dissipation during sliding results in a hysteretic "friction loop". The half-width of the friction loop (ΔV_L) is proportional to the sliding resistance (friction) force at the interface.[9] A desirable calibration constant for an LFM friction measurement could be called a "torque sensitivity" (S_T) which describes a given lateral output (ΔV_L) for a known torsional moment (T) applied to the cantilever, such that

$$S_T = \frac{\Delta V_L}{T} \tag{1}$$

In this way, when a torque is applied to the cantilever during an LFM friction measurement via a lateral friction force (F_y) applied to the cantilever in the y-direction (see Figure 1), we can quantify the force such that

$$F_y = \frac{\Delta V_L}{S_T h} \tag{2}$$

where h is the torque arm probe length from the torsional axis of the cantilever (about which twisting occurs) to the point at which force is applied at the probe−surface interface.

In addition to application of a lateral friction force (F_y) to the probe during an LFM experiment, there is always some force, F_z, applied normal to the surface plane in the z-direction (see Figure 1), where F_y is often interpreted as a function of F_z. To

*To whom correspondence should be addressed. E-mail: mark.reitsma@nist.gov.

(1) Ducker, W. A.; Senden, T. J.; Pashley, R. M. *Nature* **1991**, *353*, 239.
(2) Kappl, M.; Butt, H. J. *Part. Part. Syst. Charact.* **2002**, *19*(3), 129.
(3) Cain, R. G.; Page, N. W.; Biggs, S. *Phys. Rev. E* **2000**, *62*(6), 8369.
(4) Berg, I. C. H.; Rutland, M. W.; Arnebrant, T. *Biofouling* **2003**, *19*(6), 365.
(5) Varenberg, M.; Etsion, I.; Halperin, G. *Tribol. Lett.* **2005**, *18*(4), 493.
(6) Feiler, A. A.; Jenkins, P.; Rutland, M. W. *J. Adhes. Sci. Technol.* **2005**, *19*(3−5), 165.
(7) Pettersson, T.; Naderi, A.; Makuska, R.; Claesson, P. M. *Langmuir* **2008**, *24*(7), 3336.
(8) Cardenas, M.; Valle-Delgado, J. J.; Hamit, J.; Rutland, M. W.; Arnebrant, T. *Langmuir* **2008**, *24*(14), 7262.
(9) Ralston, J.; Larson, I.; Rutland, M. W.; Feiler, A. A.; Kleijn, M. *Pure Appl. Chem.* **2005**, *77*(12), 2149.

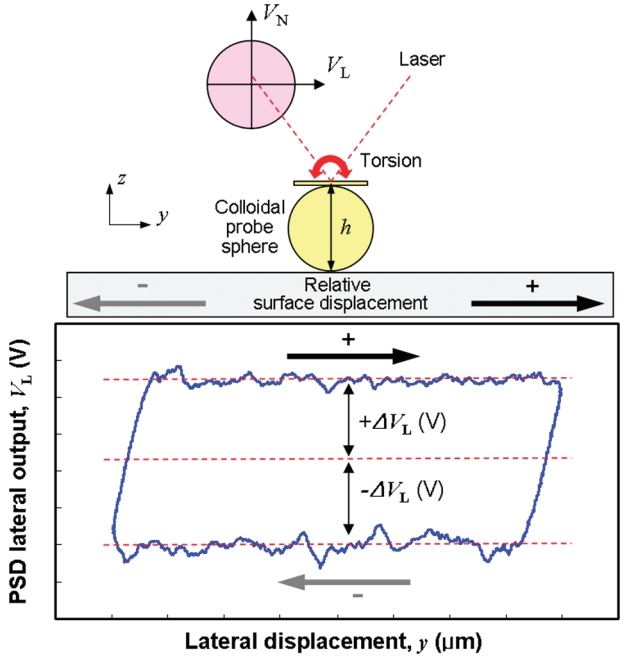

Figure 1. Front-view illustration (looking from the free end down the long axis of the colloidal probe cantilever) of a typical LFM measurement, where force is applied in the y-direction and the cantilever twists about its long (x) axis. The quadrant position sensitive photodetector (PSD) of the AFM is also shown with axes for normal (V_N) and lateral (V_L) output reading flexural and torsional deflection in the cantilever, respectively. Typical LFM friction data are also shown, where frictional energy dissipation during sliding results in a hysteretic friction loop. The half-width of the friction loop (ΔV_L) is proportional to the sliding resistance (friction) force at the interface.

quantify F_z forces, the AFM optical lever sensitivity (OLS) technique uses a normal displacement sensitivity (S_N) calibration to relate the output from the PSD (ΔV_N) to normal displacement (Δz) of the AFM displacement transducer (assumed to be equivalent to the flexural displacement of the cantilever when the probe is in contact with a rigid surface).[10−12] The calibration of normal force between the probe and a surface plane then requires the flexural stiffness (spring constant) of the AFM cantilever to be known, for which numerous techniques have been proposed and refined.[13−17] While the attainment of accuracy in the measurement of normal forces has notable challenges,[17−19] the approach of the OLS technique is, generally speaking, straightforward. This is not the case for the measurement of lateral (friction) forces in LFM, in which the practical realization of calibration parameters for a torsional moment applied to the cantilever is more complicated.

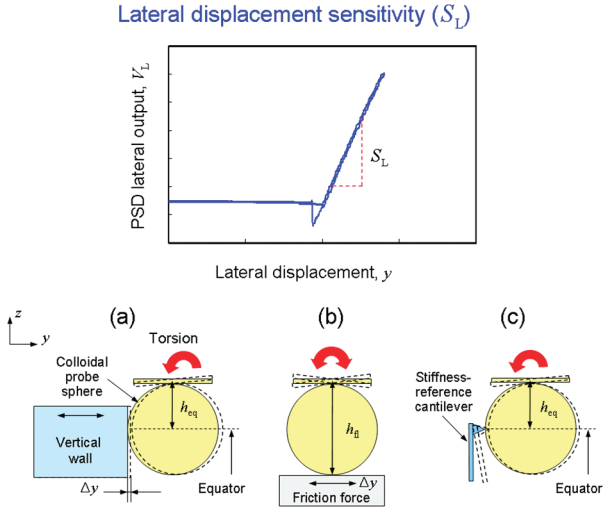

Figure 2. Front-view illustrations (looking from the free end down the long axis of the colloidal probe cantilever) of lateral displacement sensitivity loading methods, showing (a) equatorial loading, (b) frictional loading, and (c) loading against a stiffness reference cantilever. The representative lateral displacement sensitivity calibration ($S_L = \Delta V_L/\Delta y$) data shown are typical for a probe undergoing equatorial loading.

One LFM calibration approach has been to monitor the PSD response for a torque applied to the cantilever via a beam attached orthogonal to the long axis of the cantilever (and probe).[20,21] A disadvantage of this technique is that calibration and friction measurements cannot be performed in situ, as the beam needs to be either attached (or removed) between one procedure and the other, except if the beam is attached symmetrically across the cantilever.[22] The so-called wedge LFM calibration method involves sliding the cantilever probe over a surface slope of well-characterized geometry, where the mechanical response of the cantilever probe on the surface incline is understood in terms of force balance equilibrium. This technique, proposed by Ogletree et al.[23] and modified for use with colloidal probes by Varenburg et al.,[24] is not investigated in this work. We also acknowledge the potential of a direct force calibration technique using a diamagnetic levitation device, as proposed by Li et al.,[25] which is also not investigated in this paper.

The microsized sphere of a colloidal probe provides a relatively convenient means of facilitating the application of lateral forces in LFM calibration. Figure 2 shows front-view illustrations (looking from the free end down the long axis of the colloidal probe cantilever) for three types of lateral loading. Since the diameter of a microsphere can be measured readily, then the lever arm length (h_{eq}) can also be determined by carefully aligning a rigid vertical sidewall material for contact with the sphere equator, as illustrated in Figure 2a,[26,27] where torque is induced in the cantilever by scanning laterally (Δy). The representative (S_L) data shown in Figure 2 are typical for this type of loading, here termed "equatorial loading". Figure 2b shows the approach of Cain et al.,[28] who take

(10) Butt, H.-J.; Cappella, B.; Kappl, M. *Surf. Sci. Rep.* **2005**, *59*, 1.
(11) Since an AFM cantilever is usually mounted at a small angle relative to a nominal planar surface, a geometrical correction is required to resolve force in the z-direction. For example, see ref 12.
(12) Edwards, S. A.; Ducker, W. A.; Sader, J. E. *J. Appl. Phys.* **2008**, *103*, 064513.
(13) Cleveland, J. P.; Manne, S.; Bocek, D.; Hansma, P. K. *Rev. Sci. Instrum.* **1993**, *64*(2), 403.
(14) Green, C. P.; Lioe, H.; Cleveland, J. P.; Proksch, R.; Mulvaney, P.; Sader, J. E. *Rev. Sci. Instrum.* **2004**, *75*(6), 1988.
(15) Burnham, N. A.; Chen, X.; Hodges, C. S.; Matei, G. A.; Thoreson, E. J.; Roberts, C. J.; Davies, M. C.; Tendler, S. J. B. *Nanotechnology* **2003**, *14*(1), 1.
(16) Ying, Z. C.; Reitsma, M. G.; Gates, R. S. *Rev. Sci. Instrum.* **2007**, *78*, 063708.
(17) Gates, R. S.; Reitsma, M. G. *Rev. Sci. Instrum.* **2007**, *78*, 086101.
(18) Gates, R. S.; Pratt, J. R. *Meas. Sci. Technol.* **2006**, *17*, 2852.
(19) Chung, K.-H.; Shaw, G. A.; Pratt, J. R. *Rev. Sci. Instrum.* **2009**, *80*(6), 065107.
(20) Toikka, G.; Hayes, R. A.; Ralston, J. *J. Adhes. Sci. Technol.* **1997**, *11*(12), 1479.
(21) Feiler, A.; Attard, P.; Larson, I. *Rev. Sci. Instrum.* **2000**, *71*(7), 2746.
(22) Reitsma, M. G. *Rev. Sci. Instrum.* **2007**, *78*, 106102.
(23) Ogletree, D. F.; Carpick, R. W.; Salmeron, M. *Rev. Sci. Instrum.* **1996**, *67*(9), 3298.
(24) Varenberg, M.; Etison, I.; Halperin, G. *Rev. Sci. Instrum.* **2003**, *74*(7), 3362.
(25) Li, Q.; Kim, K.-S.; Rydberg, A. *Rev. Sci. Instrum.* **2006**, *77*, 065105.
(26) Ecke, S.; Raiteri, R.; Bonaccurso, E.; Reiner, C.; Deiseroth, H.-J.; Butt, H.-J. *Rev. Sci. Instrum.* **2001**, *72*(11), 4164.
(27) Cannara, R. J.; Eglin, M.; Carpick, R. W. *Rev. Sci. Instrum.* **2006**, *77*, 053701.
(28) Cain, R. G.; Biggs, S.; Page, N. W. *J. Colloid Interface Sci.* **2000**, *227*, 55.

advantage of the relatively large contact area produced by the spherical probe on a surface. At appropriately high normal loads, the probe−surface contact can be noncompliant compared to the cantilever, allowing for practically all deflection to occur in the cantilever during lateral scanning. This is here termed "frictional loading". In both frictional (where $h = h_{fl}$) and equatorial (where $h = h_{eq}$) loading, the lateral deflection response of the PSD (ΔV_L) is observed as a function of lateral displacement (Δy) of the instrument displacement transducer, such that a lateral displacement sensitivity ($S_L = \Delta V_L/\Delta y$) is observed. The idea behind these methods is that for a known torque arm length (h), the lateral displacement (Δy) can be equated to a torsional deflection in the cantilever (ϕ) (such that $\phi = \Delta y/h$, for small ϕ). It then follows that knowledge of the torsional stiffness (spring constant) of the cantilever (k_ϕ) will complete the friction force (F_y) calibration (such that $F_y = k_\phi\phi/h$).[27,28] The drawback is that cantilever torsional stiffness is a very difficult property to measure.[29]

Ecke et al.[26] circumvented the need to measure cantilever torsional stiffness by realizing force via a stiffness reference cantilever (a cantilever of predetermined flexural stiffness). Reference cantilevers were initially proposed as a means of calibrating the flexural stiffness of AFM cantilevers[30−33] and have since been considered as potential transfer artifacts for Système International d'Unités (SI)-traceable flexural stiffness determination.[17,18,34] Using a stiffness reference cantilever, flexural stiffness is measured by pressing the unknown cantilever (to be calibrated) against the stiffness reference cantilever and comparing the S_N for this interaction to the S_N obtained when the unknown cantilever is pressed against a rigid surface.[17,31−33] The analogous technique for an LFM calibration would be to compare the S_L of the loading condition shown in Figure 2a to that for loading shown in Figure 2c. For future reference, we describe the loading techniques shown in Figure 2 as displacement-based methods.

Recently, a piezo-resistive cantilever was used as a reference artifact to calibrate the flexural stiffness of AFM cantilevers, where the cantilever and its accompanying electronics form a piezo-resistive sensor so that voltage output can be related to applied force.[34] Illustrated in Figure 3a, the use of a piezo-resistive cantilever offers a direct LFM calibration for colloidal probes, giving a lateral force sensitivity ($S_{LF} = \Delta V_L/\Delta F_y$). In this case, for a known torque arm length (h_{eq}), we can convert the S_{LF} observation to a torque sensitivity (for calibration of friction data, see eq 1) such that $S_T = S_{LF}/h_{eq}$. In related work, a piezo-reference cantilever has been proposed as an LFM calibration method for cantilevers with integrated tips;[35] this approach is problematic in terms of alignment, positioning, and the determination of the contact point (i.e., to determine h) of the reference cantilever on the integrated tip of the cantilever to be calibrated (other issues like contact slippage during loading could also be problematic). For colloidal probes, however, where h_{eq} can be determined with reasonable accuracy, the piezo-resistive reference cantilever technique represents a direct force LFM calibration

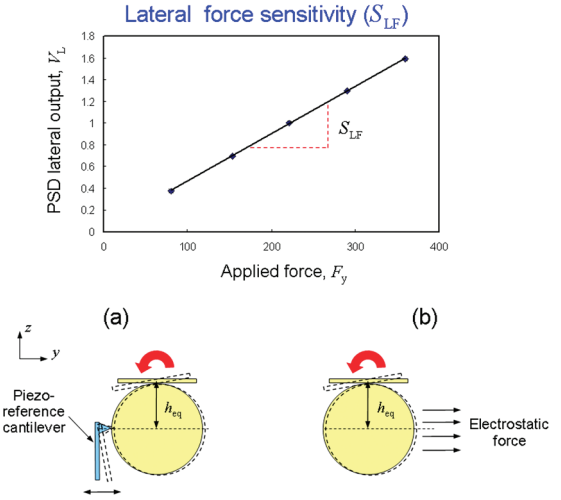

Figure 3. Front-view illustrations (looking from the free end down the long axis of the colloidal probe cantilever) of lateral force sensitivity methods, showing (a) loading against a piezo-resistive reference cantilever and (b) electrostatic loading. Representative lateral force sensitivity calibration ($S_{LF} = \Delta V_L/\Delta F_y$) data are also shown.

method, in which a calculable (precalibrated) force can be applied directly to the probe.

The purpose of this paper is to address the issue of lateral force calibration for colloidal probes by examining direct force calibration techniques (Figure 3) as well as the more commonly used displacement-based methods (Figure 2). All experiments in this work were performed using the same colloidal probe and the same LFM instrument, described in section 2. In section 3, lateral displacement sensitivity calibration methods are performed and discussed. In section 4, a new direct lateral force calibration method is introduced (illustrated in Figure 3b), where known electrostatic forces are applied to the conductive colloidal probe. In section 5, a direct force method using a precalibrated piezo-resistive cantilever is performed along with a displacement-based method, which uses the piezo-resistive reference cantilever as a stiffness reference cantilever.

2. Materials

All experiments were performed using an MFP3D AFM (Asylum Research, Santa Barbara, CA).[36] The colloidal probe used in experiments was a 51 ± 1 μm diameter polystyrene sphere (DRI-CAL Particle Size Standards, Duke Scientific), attached to a rectangular silicon nitride cantilever (MLCT-B, Veeco Probes) with approximate length, width, and thickness dimensions of 212.7 μm (L^*), 20.5 μm (w), and 0.75 μm (t), respectively (L^* is the effective length of the cantilever, from the fixed end to the center of the spherical probe). Sphere and cantilever dimensions were determined by scanning electron microscopy. The sphere was attached to the cantilever using a conductive epoxy (H21D, Epotek Technologies), and following curing, the entire probe cantilever was sputter coated with a chromium adhesion layer (approximately 5 nm) and then a gold layer (approximately 50 nm). The polystyrene spheres used here were chosen because of their highly uniform spherical shape, which is important for accurate capacitance measurements that are performed in experiments described in section 4. The mechanical stiffnesses of the

(29) The torsional Sader method[14] is a generally accepted technique for the measurement of AFM cantilever torsional stiffness. It applies to certain rectangular cantilevers but is not strictly applicable to colloidal probes. The torsional Cleveland method[14] may be applicable to colloidal probes, although the method was not used here.

(30) Rabinovich, Y. I.; Yoon, R.-H. *Langmuir* **1994**, *10*, 1903.
(31) Torii, A.; Sasaki, M.; Hane, K.; Shigeru, O. *Meas. Sci. Technol.* **1996**, *7*, 179.
(32) Gibson, C. T.; Watson, G. S.; Myhra, S. *Nanotechnology* **1996**, *7*, 259.
(33) Tortonese, M.; Kirk, M. D. *Proc. SPIE-Int. Soc. Opt. Eng.* **1997**, *3009*, 53.
(34) Langlois, E. D.; Shaw, G. A.; Kramar, J. A.; Pratt, J. R.; Hurley, D. C. *Rev. Sci. Instrum.* **2007**, *78*, 093705.
(35) Xie, H.; Vitard, J.; Haliyo, S.; Régnier, S.; Boukallel, M. *Rev. Sci. Instrum.* **2008**, *79*, 033708.

(36) Certain commercial equipment, instruments, or materials are identified in this article to adequately specify the experimental procedure. Such identification does not imply recommendation or endorsement by the National Institute of Standards and Technology, nor does it imply that the materials or equipment identified is necessarily the best available for the purpose.

polystyrene spheres used here were measured to be approximately 1.2 kN/m (using an instrumented indenter),[19] which is ~3 orders of magnitude (or more) larger than any relevant stiffness property of the cantilever used in this work. All experiments were performed in a temperature-controlled (20 ± 0.1 °C) environment.

3. Lateral Displacement Sensitivity Measurements

To perform a lateral displacement sensitivity (S_L) calibration, the colloidal probe is loaded in rigid contact while the PSD lateral output response from the AFM (V_L) is observed as a function of Δy displacement, as described earlier. Displacement can be induced via equatorial loading, shown in Figure 2a, or via frictional loading, shown in Figure 2b. Note that the lateral displacement sensitivity ($S_L = \Delta V_L/\Delta y$) data shown in Figure 2 are typical for equatorial loading. It is important to note that the three lateral force calibration methods performed in this work, the two direct force methods (Figure 3) and the stiffness reference cantilever method (Figure 2a,c), are each carried out by loading the colloidal probe sphere at its equator (i.e., equatorial loading). On the other hand, frictional loading (Figure 2b) is clearly relevant to the actual conditions experienced by the colloidal probe during a friction measurement. In this section, we compare the equatorial loading condition to that of frictional loading in terms of respective S_L measurements.

A lateral force applied in the y-direction through a torque arm (probe) length (h) will deflect a colloidal probe cantilever of torsional stiffness k_ϕ via twisting (rotating) about its long (x) axis through an angle ϕ such that we can describe a torque ($T = k_\phi\phi$). From this, we can define a "torque arm stiffness" (k_T) such that[27,28]

$$k_T = \frac{k_\phi}{h^2} \tag{3}$$

where $h = h_{eq} = R + t/2$ for equatorial loading and $h = h_{fl} = 2R + t/2$ for frictional loading; R is the colloidal probe sphere radius, and t is the cantilever thickness.[37] The lateral displacement sensitivity methods shown in Figure 2 share an important assumption, which is that the only "lateral spring" in the colloidal probe system is the torsional spring (stiffness) of the cantilever. However, the lateral loads experienced by a cantilever during both frictional and equatorial loading also cause deflection of the cantilever in the $x-y$ plane (the "in-plane") direction. This means that the total lateral stiffness of the cantilever (k_{lat}) will consist of both an in-plane cantilever stiffness (k_{ip}) and the torque arm stiffness (k_T) (eq 3), such that

$$k_{lat} = \left(\frac{1}{k_T} + \frac{1}{k_{ip}}\right)^{-1} \tag{4}$$

Beam theory predicts the ratio of these springs to be[27,38]

$$\frac{k_T}{k_{ip}} = \left[\frac{2}{3(1+\nu)}\right]\left(\frac{t}{h}\right)^2\left(\frac{L^*}{w}\right)^2 \tag{5}$$

where ν is the Poisson's ratio of the cantilever beam material. It turns out that many commercially available rectangular AFM cantilevers will exhibit significant in-plane deflection when loaded laterally. The problem for lateral displacement sensitivity measurements is that the PSD of the AFM is practically insensitive to in-plane cantilever deflection. The consequence of this is an underestimation of the lateral displacement sensitivity calibration parameter (S_L), since the displacement transducer is deflecting two springs (k_T and k_{ip}), whereas the PSD is accounting for the deflection of only one (k_T). For the colloidal probe used in this work, the proportion of in-plane deflection to total lateral deflection is estimated to be 4.5% for equatorial loading and 1% for frictional loading (using eq 5). Note that to observe the effect of in-plane deflection on the calibration methods discussed in this paper, we ignore the contribution from in-plane deflection (i.e., we assume that $k_{ip}^{-1} = 0$) when calculating cantilever lateral stiffness (k_{lat}), as discussed later. Another spring in the colloidal probe system that can contribute to an underestimation of the S_L parameter is the glue joint between the sphere and cantilever. Using analysis described elsewhere,[28] the compliance of the glue joint used in this work was estimated to be at least 3 orders of magnitude smaller than that of the lateral compliance of the cantilever (k_T^{-1}). The glue joint is thus expected to have a negligible effect on the observed S_L for both frictional and equatorial loading cases here. Finally, although the frictional loading condition is apparently less susceptible to in-plane cantilever deflection compared to equatorial loading (due to a longer torque arm, h), frictional loading has its own additional (spring deflection) susceptibility, which is discussed in the following section.

3.1. Frictional Loading. Carpick et al.[39] pointed out that the finite contact area between an AFM probe and surface can be subject to significant deformation during frictional loading. In some cases, the lateral stiffness of a probe−surface contact (k_{clat}) can be comparable to the lateral stiffness of the cantilever. This means that if frictional loading is used to generate a lateral displacement sensitivity for a lateral force calibration, as in the approach of Cain et al.,[28] then materials and conditions need to be optimized such that the probe−surface contact compliance is minimized. We can describe the combined lateral stiffness of the cantilever−probe−surface system in frictional loading as $k_{lat} = (k_T^{-1} + k_{ip}^{-1} + k_{clat}^{-1})^{-1}$. As demonstrated by Cain et al.,[28] if appropriate (large Young's modulus) sphere and surface materials are used, the combined stiffness of the system asymptotes to the cantilever springs $[(k_T^{-1} + k_{ip}^{-1})^{-1}]$ since k_{clat}^{-1} will approach zero at suitably large normal applied loads.

Figure 4a shows a friction loop, acquired while sliding the colloidal probe used here on a silicon (100) surface. The lateral displacement sensitivity for frictional loading (S_L^{fl}) is obtained from the linear slope in the "static friction" portion of the friction trace, where S_L^{fl} is taken to be the average of slopes for sliding in one direction ($S_{L,left}^{fl}$) and then the reverse ($S_{L,right}^{fl}$). Figure 4b shows the effect of contact stiffness on the determination of S_L^{fl}. In this example, S_L^{fl} can be seen to asymptote to a value of approximately 3.2 mV/nm for applied normal loads above ~25 μN. At these loads, k_{clat} is predicted to be at least 3 orders of magnitude greater than k_T (based on Hertzian contact mechanics).[40] The S_L^{fl} value used in this work was measured at normal applied loads of 35 μN, averaged from the slopes at both ends of each friction loop, where the mean value

(37) The torsional axis of the cantilever is assumed to be aligned down the long (x) axis and centered through the thickness and width of the cantilever. It is acknowledged that this assumption may not be strictly correct for all loading conditions, as pointed out in ref 25.

(38) Sader, J. E.; Green, C. P. *Rev. Sci. Instrum.* **2004**, *75*(4), 878.

(39) Carpick, R. W.; Ogletree, D. F.; Salmeron, M. *Appl. Phys. Lett.* **1997**, *70* (12), 1548.

(40) Johnson, K. L. *Contact Mechanics*; Cambridge University Press: Cambridge, U.K., 1987.

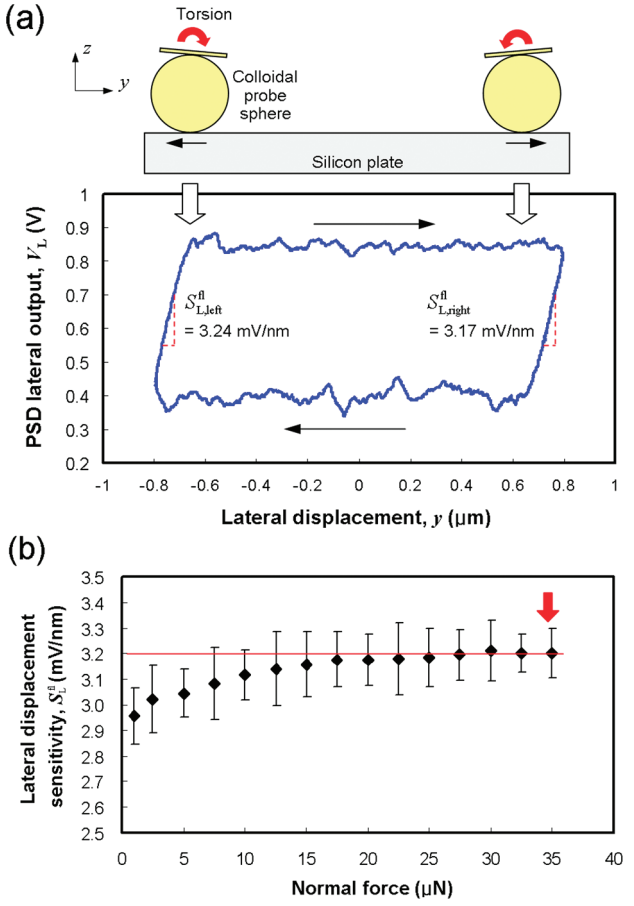

Figure 4. Frictional loading data, showing (a) a friction loop acquired while sliding the colloidal probe on a crystalline silicon surface, in which a lateral displacement sensitivity (S_L^{fl}) measurement is taken from the static friction portions of the loop and (b) the effect of contact stiffness on the S_L^{fl} measurement, where an asymptote can be seen for loads above ~25 μN. In this case, the probe−contact lateral stiffness (k_{clat}) is predicted to be more than 3 orders of magnitude greater than the torque arm stiffness (k_T) of the cantilever, based on Hertzian contact mechanics.

of S_L^{fl}, taken from 10 repeated measurements, was 3.2 ± 0.1 mV/nm.[41]

3.2. Equatorial Loading. Because of the large stiffness of a compressively loaded, as opposed to a sheared, contact, the contact compliance issue that is relevant to frictional loading is not typically an issue for equatorial loading (except for very soft sphere materials).[39,40] To load the sphere of the colloidal probe, the edge of a silicon AFM cantilever (die) chip was used rather than a vertical walled crystal, as used by Cannara et al.[27] Because of this, we implemented an alignment protocol to establish the position of loading at the equator of the colloidal probe sphere. Shown in Figure 5a, closed loop z-displacement between the sphere and chip is plotted on the abscissa and the observed S_L is plotted on the left ordinate axis; closed loop y-displacement at initial contact (snap-in) is plotted on the right ordinate axis. Alignment in x was conducted using the overhead optical microscope of the AFM. From Figure 5a, the expected linear relationship between S_L and z-displacement is represented by the filled diamonds. The open diamonds represent closed loop y-displacement at initial (snap-in)

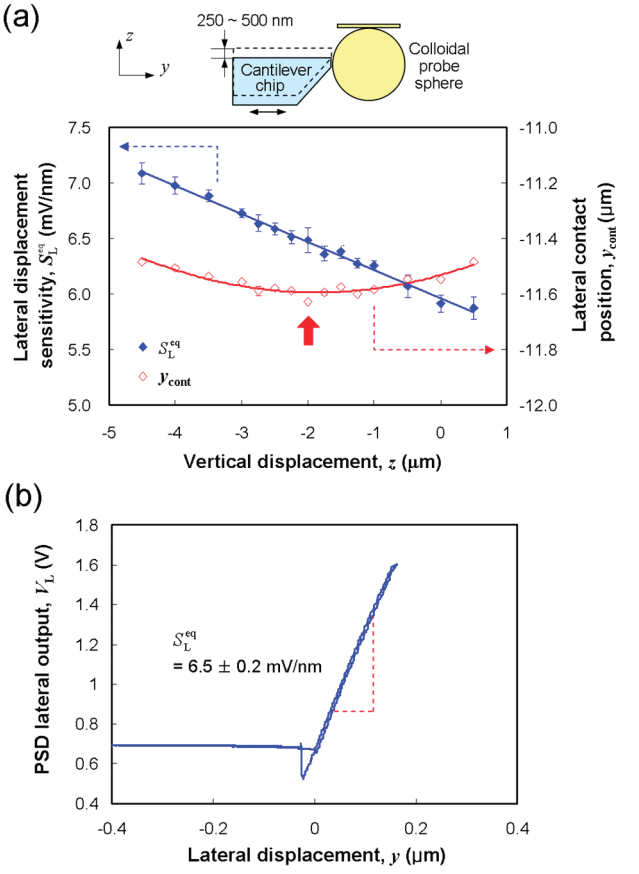

Figure 5. Representative data for the lateral alignment protocol used here for equatorial displacement-based loading of the colloidal probe sphere against a rigid material (AFM cantilever chip). (a) Expected linear relationship of S_L^{eq} as a function of z-displacement (◆). Also shown is closed loop y displacement at initial contact (snap-in) (y_{cont}) between the ramp chip and spherical probe (◇), representing the spherical shape of the probe. (b) Representative lateral displacement sensitivity data.

contact (y_{cont}) between the ramp chip and spherical probe as a function of closed loop z-displacement, which shows an anticipated circular shape representing the spherical shape of the probe. The lateral displacement sensitivity values used for S_L^{eq} were taken from the minimum y_{cont} value in Figure 5a. A representative lateral displacement sensitivity S_L^{eq} of 6.5 ± 0.2 mV/nm was determined from the average of linear curve fitting of 10 repeat S_L^{eq} observations.[41]

3.3. Lateral Displacement Sensitivity Comparison. To compare S_L values from frictional and equatorial loading, results were normalized by taking the product of S_L values and their respective h values. The in situ comparison of loading techniques conducted here gave an equatorial loading value ($h_{eq}S_L^{eq}$) of 168 ± 7 V, which was in agreement with the frictional loading value ($h_{fl}S_L^{fl}$) of 164 ± 8 V (within 3%).[41,42] Equation 5 predicts an approximate 3.5% difference between frictional and equatorial loading because of the differing degrees of in-plane cantilever deflection. The discrepancy falls within uncertainty limits for these observations. The agreement between S_L values provides validation for the assumption that equatorial loading is a good representation of frictional loading for the purposes of calibrating LFM friction data. The following sections describe lateral force calibration methods that load the colloidal probe sphere via its equator.

(41) Unless otherwise stated, all uncertainties represent one standard deviation.

(42) Value includes uncertainty in the determination of h (which was ±250 nm).

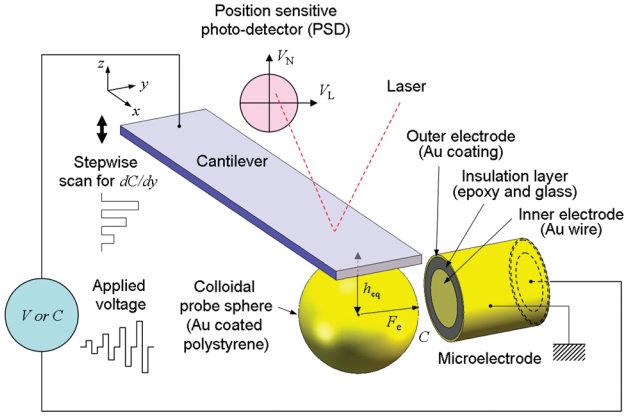

Figure 6. Schematic of the experimental setup for the application of lateral electrostatic force to a conductive colloidal probe.

4. Electrostatic Lateral Force Calibration

An accurate method for applying calculable electrostatic forces to a conductive colloidal probe has been demonstrated recently by Chung et al.[19] The technique eliminates the need to evaluate displacement sensitivity or the colloidal probe's flexural stiffness to obtain a force measurement, and forces applied to the colloidal probe can be determined with an accuracy of 2%, traceable to the SI. Illustrated in Figure 6, the same experimental setup has been configured for LFM calibration, such that the electrode was positioned orthogonal to the long axis of the cantilever (x) and probe (z). The microelectrode was prepared using a gold microwire (California Fine Wires),[36] inserted into a glass micropipet and secured using epoxy. Alignment between the electrode and the center of the sphere was determined from the maximum capacitance obtained at the sphere equator (at torque arm distance h_{eq}) using an alignment technique described elsewhere.[19] Once alignment had been achieved, the gap between the sphere and the electrode was decreased until a measurable capacitance gradient could be obtained. Using a closed loop lateral displacement transducer, the capacitance gradient was measured in approximately 20 nm increments over a total distance of ~140 nm. Between the increments, the applied voltage was set back to zero to monitor the baseline and correct for drift. After characterization of the capacitance gradient, torsional deflection in the cantilever was induced using stepwise voltages (from 0 to 16 V) applied between the probe and the electrode. The surface potential between the probe and electrode was measured by applying voltages with opposite polarities and monitoring the response of the probe via the PSD of the AFM. In this case, the surface potential (U_S) was calculated to be 0.19 ± 0.02 V. The applied electrostatic force (F_e) was determined by

$$F_e = \frac{1}{2}\frac{dC}{dy}(U^2) \tag{6}$$

where C is the capacitance, y is the closed loop lateral displacement, and U is the potential. Figure 7a shows the capacitance trend with lateral displacement over a distance of approximately 140 nm. The relation between C and y appears to be linear, giving a capacitance gradient of dC/dy of 1.11 ± 0.02 fF/m, obtained from the average slope (mean ± one standard deviation) using least squares curve fits of five repeated data sets. The residuals plotted in the inset of Figure 7a indicate that no significant nonlinearity was observed over the course of the measurement.

After characterizing the electrostatics of the system, we applied a known electrostatic force (F_e) to the colloidal probe while

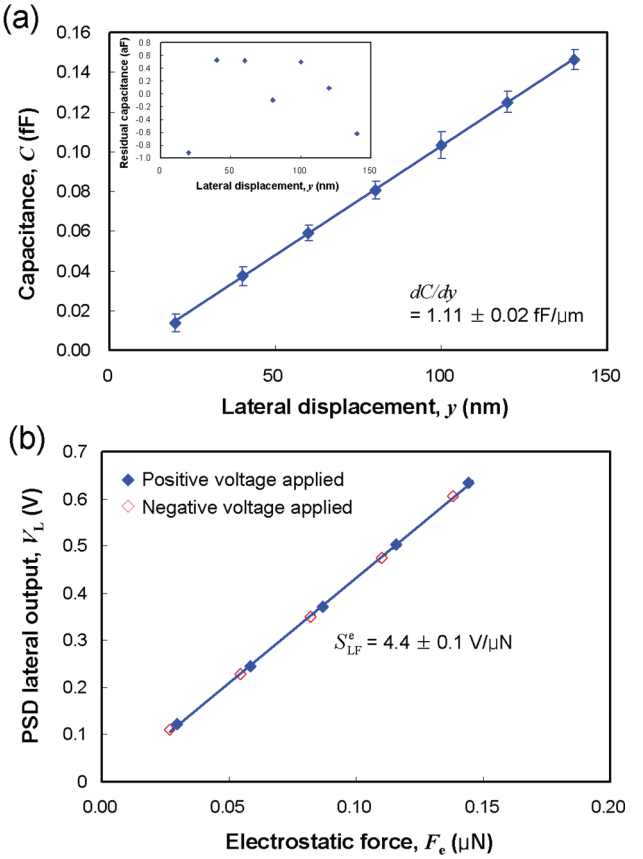

Figure 7. Electrostatic measurements between the conductive colloidal probe and microelectrode: (a) capacitance gradient (dC/dy) obtained for the experimental setup used here (inset shows no significant systematic uncertainty over the course of the measurement) and (b) lateral force sensitivity obtained by applying electrostatic force directly to the conductive colloidal probe.

monitoring the lateral PSD response (ΔV_L). We describe the electrostatic lateral force sensitivity (S^e_{LF}) as

$$S^e_{LF} = \frac{\Delta V_L}{F_e} \tag{7}$$

The calibration plot for this relationship is shown in Figure 7b, where the S^e_{LF} of 4.4 ± 0.1 mV/nN was determined by least-squares fitting from five repeated measurements (uncertainty includes the positioning uncertainty in the z-direction during the calibration).[41,42] In section 1, we discuss the torque sensitivity parameter (S_T) (eq 1), used to scale friction loop data and thus quantify lateral (friction) forces in LFM. Using the electrostatic lateral force sensitivity (S^e_{LF}) obtained above and an h_{eq} of 25.9 ± 0.7 μm from SEM, we calculate the torque sensitivity of this system as $S^e_T = S^e_{LF}/h_{eq}$ = 172 ± 7 V/nNm, where the largest uncertainty in this measurement is positioning uncertainty in the z-direction during the calibration.[41,42]

In the same experiment, a lateral displacement sensitivity was performed (see section 3.2), which gave an S^{eq}_L value of 6.5 ± 0.2 mV/nm. Using this value, the lateral stiffness of the colloidal probe loaded (electrostatically) at its equator is calculated as

$$k^e_{lat} = \frac{S^{eq}_L}{S^e_{LF}} \tag{8}$$

giving a k_{lat}^{e} value of 1.46 ± 0.07 N/m. Note that we are absorbing the systematic error from in-plane displacement of the cantilever in the S_L^{eq} measurement by assuming that $k_{lat} = k_T$ (i.e., that $k_{ip}^{-1} = 0$ in eq 4), which was described earlier (and will be discussed later).

The method described here is a direct lateral force calibration for conductive colloidal probes that uses SI-traceable electrostatic forces. In the following section, we describe methods that apply forces to the colloidal probe sphere using a calibrated reference cantilever.

5. Reference Cantilever Lateral Force Calibration

In this section, a piezo-resistive cantilever is used as both a stiffness reference artifact and a force reference to perform lateral force calibration measurements on the colloidal probe cantilever. The rectangular-shaped piezo-resistive reference cantilever (FMT-400, Kleindiek Nanotechnik)[36] had nominal dimensions of 400, 50, and 4 μm for length, width, and thickness, respectively. The integrated tip of the cantilever had a height of approximately 5 μm. SI-traceable forces were applied to the piezo-resistive reference cantilever using the National Institute of Standards and Technology (NIST) Electrostatic Force Balance (EFB). Forces were applied while both cantilever flexural deflection (interferometry) and piezo-resistance (Agilent 3458A, Agilent Technologies, Inc.)[36] were monitored versus applied load using techniques described elsewhere,[43] where all measurements were SI-traceable. The flexural stiffness of the piezo-resistive reference cantilever (k_{REF}) was measured to be 1.846 ± 0.005 N/m with a resistive sensitivity (S_r) of 1.121 ± 0.002 Ω/μN.

To perform lateral reference cantilever measurements on the colloidal probe, we first used the piezo-resistive reference cantilever as a stiffness reference artifact and then as a force reference device. The reference cantilever was mounted and glued against a vertical sidewall, which was then placed in the AFM experimental setup such that the long axis of the cantilever was along the z-axis. For both types of measurement, the contact position of the reference cantilever on the sphere was determined using the same alignment protocol as described in section 3.2 (see also Figure 5a), but in this case, alignment was performed in the x-direction as well as the z-direction. It should be noted that following the electrostatic calibration in section 4, the colloidal probe was remounted in the AFM cantilever holder in preparation for the experiments described in this section. The remounted system gave an S_L^{eq} of 6.4 ± 0.2 mV/nm, determined from the average value of approach and retract data for 10 repeated measurements[41,42] [the previous value was 6.5 ± 0.2 mV/nm (see section 3.2)].

5.1. Stiffness Reference Cantilever Calibration. A stiffness reference calibration was performed by comparing the lateral displacement sensitivity for the colloidal probe loaded against a rigid material (S_L^{eq}) to that for the colloidal probe loaded against the stiffness reference cantilever (S_L^{sr}). The lateral stiffness of the colloidal probe (k_{lat}) is given as

$$k_{lat}^{sr} = k_{REF}\left(\frac{S_L^{eq}}{S_L^{sr}} - 1\right) \tag{9}$$

Representative data are shown in Figure 8, where S_L^{sr} = 3.5 ± 0.1 mV/nm and S_L^{eq} = 6.4 ± 0.2 mV/nm. From eq 9, the lateral stiffness of the colloidal probe (k_{lat}^{sr}) was determined to be 1.54 ± 0.07 N/m, from the average of 10 repeated measurements.[41,42] The lateral force sensitivity of the optical lever system is

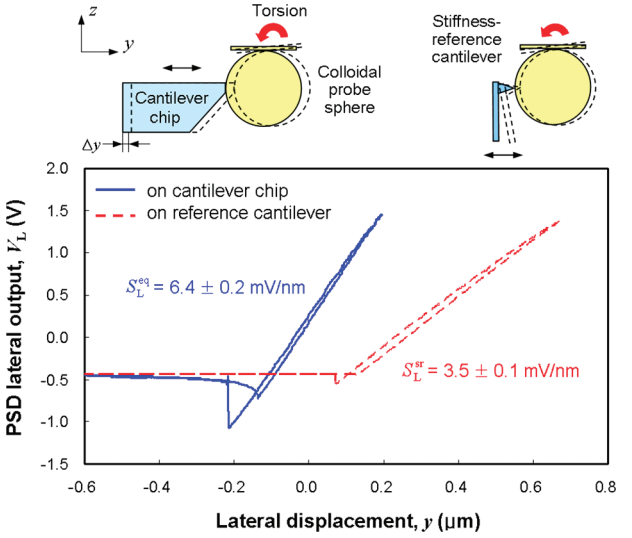

Figure 8. Representative data for the stiffness reference calibration method.

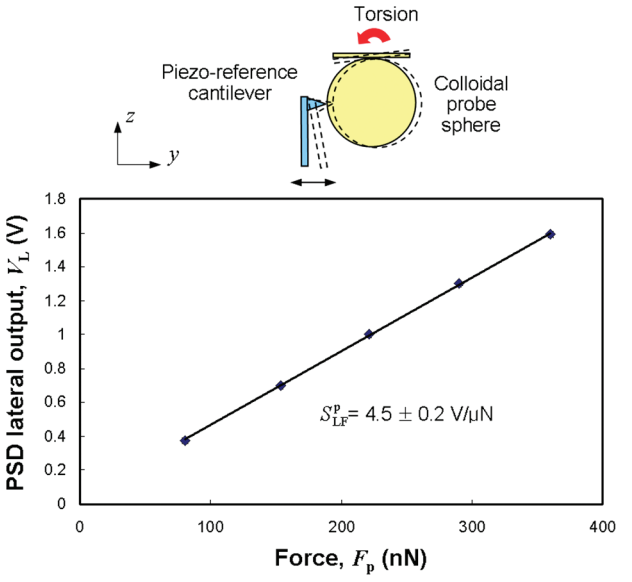

Figure 9. Representative data for the piezo-resistive reference cantilever method.

calculated as

$$S_{LF}^{sr} = \frac{S_L^{eq}}{k_{lat}^{sr}} \tag{10}$$

which gave an S_{LF}^{sr} of 4.2 ± 0.2 mV/nN. The torque sensitivity of the system [used to quantify friction data (see eq 1)] was calculated to be $S_T^{sr} = S_F^{sr}/h_{eq}$ = 160 ± 10 V/nNm.

5.2. Direct Piezo-Resistive Reference Cantilever Calibration. The electrostatic lateral force calibration in section 4 is a direct force calibration, where PSD output is observed for a known force applied directly to the torque arm (probe) of the colloidal probe. We now compare this with another direct force method using the calibrated piezo-resistive reference cantilever as a piezo-resistive force transducer. Illustrated with representative output data in Figure 9, lateral force was determined from resistance output from the calibrated piezo-resistive reference cantilever when pressed against the equator of the colloidal probe sphere using the same loading technique described in section 5.1.

(43) Pratt, J. R.; Smith, D. T.; Newell, D. B.; Kramar, J. A.; Whitenton, E. *J. Mater. Res.* **2004**, *19*(1), 366.

Table 1. Summarized Calibration Results[a]

	optical lever system properties		cantilever stiffness properties	
calibration method	lateral force sensitivity S_{LF} (mV/nN)	torque sensitivity S_T (V/nNm)	lateral stiffness k_{lat} (N/m)	torsional stiffness k_ϕ (nNm/rad)
electrostatic (direct force)	4.4 ± 0.1	172 ± 7	1.46 ± 0.07	0.98 ± 0.07
stiffness reference	4.2 ± 0.2	160 ± 10	1.54 ± 0.07	1.03 ± 0.07
piezo-reference (direct force)	4.5 ± 0.2	174 ± 9	1.43 ± 0.08	0.96 ± 0.07

[a] All values are means ± the combined uncertainty (one standard deviation).

The force applied by the piezo-reference cantilever (F_p) is determined as

$$F_p = \frac{\Delta\Omega}{S_r} \tag{11}$$

where $\Delta\Omega$ is the observed change in resistance. The lateral force sensitivity is then given by

$$S_{LF}^{p} = \frac{\Delta V_L}{F_p} \tag{12}$$

The lateral force sensitivity of the colloidal probe (S_{LF}^{p}) was determined to be 4.5 ± 0.2 mV/nN, from 10 repeated measurements.[41,42] The torque sensitivity of this system is calculated as $S_T^{p} = S_{LF}^{p}/h_{eq} = 174 \pm 9$ V/nNm.

The lateral stiffness of the colloidal probe is calculated as

$$k_{lat}^{p} = \frac{S_L^{eq}}{S_F^{p}} \tag{13}$$

where $S_L^{eq} = 6.4 \pm 0.2$ mV/nm, giving a k_{lat}^{p} of 1.43 ± 0.08 N/m.

6. Discussion

We have demonstrated a direct in situ procedure for calibrating the lateral force response of an AFM by applying known electrostatic forces directly to a conductive colloidal probe. This method was compared to another direct force method on the same colloidal probe using a piezo-resistive reference cantilever as a force transducer. We have further compared these methods to a displacement-based sensitivity method using the piezo-resistive cantilever as a stiffness reference artifact. Table 1 summarizes data obtained for all three methods in terms of two general types of properties: (1) in terms of lateral force sensitivity (S_{LF}) and torque sensitivity (S_T) which are "optical lever system properties", dependent on the system optics and cantilever (e.g., cantilever mounting, spot shape and positioning on cantilever, type of PSD, etc.), and (2) in terms of cantilever lateral stiffness (k_{lat}) and torsional stiffness (k_ϕ) which are "cantilever stiffness properties". It was noted earlier that the colloidal probe used in this work was remounted between the electrostatic calibration (section 4) and the reference cantilever calibration experiments (section 5), which is a change that will affect optical lever system properties but should not affect the stiffness properties of the cantilever. As it turned out, no significant change in displacement sensitivity was observed between the electrostatic and reference cantilever experiments (compare S_L^{eq} values in section 5). As a result, lateral force sensitivity (S_{LF}) values were within experimental uncertainty for both direct force methods (see Table 1). In contrast, the displacement-based stiffness reference cantilever method gave a lateral force sensitivity value (S_{LF}) that was roughly 7% lower than the direct force method values (Table 1) due to a diminished lateral displacement sensitivity, caused by in-plane deflection in the colloidal probe cantilever during loading. The effect of in-plane cantilever deflection on displacement-based methods is discussed in section 3. If we assume a simple beam theory prediction of 4.5% for the contribution of in-plane cantilever deflection to the overall displacement of the cantilever (eq 5), the approximately 2.5% discrepancy between predicted and measured values (i.e., 4.5% vs 7%) falls within the experimental uncertainty for measurements here. This highlights the importance of the choice of materials if a displacement-based method is to be used for colloidal probe LFM calibration. In this work, by using a cantilever that undergoes a relatively small in-plane deflection during lateral loading, systematic error from in-plane deflection could be minimized within experimental random uncertainty. In contrast to displacement-based methods, in-plane cantilever deflection does not impact lateral force sensitivity values generated by direct force methods because the lateral displacement imposed on the colloidal probe is caused by a calculable force. On the other hand, the determination of cantilever spring constants (k_{lat} and k_ϕ) requires at least one displacement-based measurement (in these experiments, S_L^{eq}) for all methods. Table 1 shows lateral stiffness values (k_{lat}) measured at the sphere equator of the colloidal probe for each respective calibration method. It was mentioned earlier that the effect of in-plane deflection was ignored in the calculation of k_{lat} for each method and that the total lateral stiffness measured was assumed to be equal to the torque arm stiffness of the cantilever, k_T (i.e., $k_{ip}^{-1} = 0$ in eq 5, so that $k_{lat} = k_T$). In-plane cantilever deflection would be expected to give reduced k_{lat} values for both direct force calibration methods (electrostatic and piezo-resistive reference), since these measurements have a proportional dependence on S_L^{eq} (see eqs 8 and 13). However, for the stiffness reference method, eq 9 implies an attenuated susceptibility to in-plane deflection because the effect has contributions in both S_L^{eq} and S_L^{sr} measurements. The expected general trend is therefore to observe k_{lat} values that tend to be larger for the stiffness reference method and smaller for direct force methods. This trend is evident in Table 1. Table 1 also lists cantilever torsional stiffness values for each calibration method, which were calculated from lateral stiffness measurements, such that $k_\phi = k_{lat}(h_{eq})^2$.

Section 3 of this paper is devoted to comparing equatorial and frictional loading (displacement-based) measurements because each calibration method investigated in this work used equatorial loading to apply force to the colloidal probe, whereas frictional loading is clearly relevant to the actual conditions experienced by the colloidal probe during a friction measurement. In comparing the two loading techniques, eq 5 predicts a 3.5% difference between equatorial loading (S_L^{eq}) and frictional loading (S_L^{fl}) in terms of the contribution of in-plane cantilever deflection to a total displacement measurement. We found that the total observed discrepancy in measured values (3%) was within experimental uncertainty for the two loading techniques. On one hand, this result supports the argument that colloidal probe equatorial loading is a good representation of frictional loading for the purposes of LFM calibration. On the other hand, it demonstrates that accuracy in displacement-based sensitivity methods is limited

considerably by the materials chosen for use. In this case, the choice of cantilever determines the extent to which in-plane deflection will become an issue for displacement sensitivity measurements. The effect of in-plane deflection is minimized if frictional loading (rather than equatorial loading) is used. However, if frictional loading is chosen, then the choice of sphere material as well as flexural stiffness of the cantilever must be considered accordingly, since these properties will determine the extent to which contact stiffness between the probe and surface will act to diminish lateral displacement sensitivity measurements.

The comparison of lateral force calibration methods investigated in this work has demonstrated the direct electrostatic force calibration to be the method with the most potential for accuracy, since an accurate SI-traceable force is applied directly to the probe sphere and alignment between the sphere and electrode can be determined precisely. The flexural stiffness and resistive sensitivity of the piezo-resistive cantilever were also determined with SI-traceable accuracy; however, alignment between the cantilever and colloidal probe sphere was found to be less precise than that of the electrostatic procedure. Other than accuracy, the advantage of direct force calibration (piezo-resistive cantilever and electrostatic) methods is their immunity to in-plane cantilever deflection for determination of the torque sensitivity parameter (S_T), which quantifies LFM output data in terms of a frictional force. The displacement-based stiffness reference cantilever method, however, will always be subject to some error due to in-plane cantilever deflection (and possibly other spring displacements) in the colloidal probe mechanical system.

A practical drawback of both reference cantilever methods, at least as they were conducted here, is that care is required in the setup of the experiment, particularly with regard to cantilever alignment. Although alignment can be more precisely determined for the electrostatic method (using observable capacitance), the electrostatic method is limited by the requirement for a conductive colloidal probe. Also, with the apparatus used in this work, accuracy in the capacitance gradient measurement was limited to experiments that used spheres larger than 30 μm.

A limitation for both the electrostatic and piezo-resistive cantilever (direct force) methods is that measurements must be made in a dielectric medium, typically air. If colloidal probe friction measurements must be taken in a conductive liquid medium, the most appropriate of the methods investigated here would be an in situ stiffness reference calibration, with adequate consideration given to cantilever/probe geometry and material properties, such that the deflection of component springs (particularly in-plane cantilever deflection and deformation of the probe−surface contact) is minimized during loading.

7. Conclusions

Using a single colloidal probe, we have compared three lateral force calibration techniques for colloidal probe friction measurements in atomic force microscopy. A direct procedure was performed by application of calculable electrostatic forces to a conductive colloidal probe, and a second direct force calibration was performed using a precalibrated piezo-resistive reference cantilever. A third calibration used the piezo-resistive reference cantilever as a stiffness reference artifact. We found agreement within experimental random uncertainty for the direct force (electrostatic and piezo-resistive) methods and accounted for a systematic error due to in-plane cantilever deflection in the stiffness reference cantilever (displacement-based) method. The comparison establishes the existing limits of instrument accuracy and sets down a basis for selection criteria for materials and methods for colloidal probe friction (lateral) force measurements in atomic force microscopy. The direct force methods used here gave the most accurate calibration but were limited to experiments in dielectric media (e.g., air). The stiffness reference method is not restricted to immersion in any particular medium, but since it is a displacement-based method, adequate consideration should be given to colloidal probe materials chosen for use, particularly to minimize in-plane deflection of the cantilever and/or deformation of the probe−surface contact during loading. Notably, however, the comparison conducted here has demonstrated that a good lateral force calibration can be achieved using a stiffness reference cantilever provided adequate attention is paid to alignment issues and choice of materials used.